Available online at www.sciencedirect.com

SciVerse ScienceDirect

Ceramics International 39 (2013) 4513–4521

CERAMICS INTERNATIONAL

www.elsevier.com/locate/ceramint

Highly luminescent yttria–silica core–shell nanoparticles by the sacrificial polymer shell method

Mehdi Ghahari[a,*], Paola Fabbri[b], Francesco Pilati[b], Luca Pasquali[b], Monica Montecchi[b], Roya Aghababazadeh[c]

[a]Nanomaterials and Nanocoatings Department, Institute for Color Science and Technology (ICST) Tehran 1668814811, ICPC 16765-654, Iran
[b]Department of Materials and Environmental Engineering, University of Modena and Reggio Emilia, Strada Vignolese 905/A, 41125 Modena, Italy
[c]Inorganic Pigments and Glazes Department, Institute for Color Science and Technology (ICST) Tehran 1668814811, ICPC 16765-654, Iran

Received 18 October 2012; accepted 16 November 2012
Available online 27 November 2012

Abstract

This paper describes the correlation existing between the photoluminescence of core–shell $SiO_2@Y_2O_3:Eu^{3+}$ nanoparticles synthesised by a method based on a sacrificial polymer-shell intermediate, and the thickness of that polymer shell. The method is based on the synthesis of a covalently bonded sacrificial polymer shell by polymerization of methacryl oxyethyl isocyanate (MOI) onto silica cores; the polymer shell was demonstrated to act as a promoter and stabilizer of the adsorption of yttrium and europium ions on the surface of silica, and its thickness plays an important role on the final luminescent intensity of the hybrid particles, which is related to the adhesion and continuity of the lanthanide shell of $SiO_2@Y_2O_3:Eu^{3+}$ nanoparticles. Yttria shells were obtained with thickness varying in the range 3–20 nm by tuning the polymer shell thickness in the range 0–50 nm. Results demonstrate that photoluminescence of $SiO_2@Y_2O_3:Eu^{3+}$ nanoparticles prepared via the sacrificial polymer shell method is much higher with respect to nanoparticles obtained by a traditional procedure.

Keywords: Core–shell particles; Photoluminescence; Methacryl oxyethyl isocyanate; Yttrium oxide

1. Introduction

$Y_2O_3:Eu^{3+}$ phosphors have been widely investigated as red-emitting phosphor for many display and lighting devices [1]. Its main applications include field emission displays (FED) [2], cathode ray tubes [3], tricolor lamps [4] and plasma display panels [5].

Recently, core shell structures phosphors have attracted great attention due to their advantages such as high monodispersbility, cost reduction and crystallite size controllability [6–9]. Undoubtedly, silica is the main important material considered as core, because it is synthesized easily by the Stöber procedure [10].

So far, different procedures have been applied to the synthesis of core shell structures including spray pyrolysis [11], precipitation [12], thermal decomposition [13] and the sol–gel process [14]. But lack of shell uniformity and low degree of core coverage by shell are the main disadvantages of these methods. Controlling the shell thickness is of fundamental importance due to the fact that it directly affects the properties of the deriving core–shell particles [15,16], recently, Liu et al. [17] demonstrated that thicker shells induce the decrease of excitation power density and thus increased intensity ratio of $^5D_0$-$^7F_2$ to $^5D_0$-^7F_J (J=1,4).

On the other hand, a wide amount of literature demonstrates that silica can be easily encapsulated by homogeneous polymer shells. Several examples of in-situ polymerizations to cover silica cores with different polymer shells have been reported [18,19]. Vinyltriethoxysilane [20], methacroyloxypropyltriethoxysilane [21], methyltrimethoxysilane [22] and glycidyloxypropyltrimethoxysilane [23] are just a few examples of molecules or coupling agents which have been used for this purpose.

In this work, we have prepared $SiO_2@Y_2O_3:Eu^{3+}$ particles by the sacrificial polymer shell method that we

*Corresponding author. Tel.: +98 912 2177311; fax: +98 21 22947537.
E-mail address: maghahari@icrc.ac.ir (M. Ghahari).

0272-8842/$ - see front matter © 2012 Elsevier Ltd and Techna Group S.r.l. All rights reserved.
http://dx.doi.org/10.1016/j.ceramint.2012.11.047

recently developed [24,25]. By tuning the thickness of the sacrificial polymer shell we were able to tune the thickness and uniformity of the final Y_2O_3:Eu^{3+} layer, and hence the photoluminescence of the hybrid nanoparticles.

2. Experimental

2.1. Materials

High purity raw materials for the synthesis of silica particles (tetraethyloxsilane 99% (TEOS), absolute ethanol (EtOH), ammonia 28% ($NH_3 \cdot H_2O$)), Y_2O_3 (99.99%), Eu_2O_3 (99.99%), HNO_3, trimethoxysilyl propyl methacrylate (MPS), methacryl oxyethyl isocyanate (MOI), tetrahydrofuran (THF), 2,2′-azobisisobutyronitrile (AIBN)), were all obtained from Merck to Sigma-Aldrich (Milan, Italy) and used as received.

2.2. Preparation of silica particles encapsulated in the polymer shell

Silica particles encapsulated in a sacrificial polymer shell were prepared following a previously reported method [24,25]. Briefly, monodispersed spherical silica nanoparticles were prepared according to the Stöber procedure and surface functionalization by MPS was used to introduce vinyl groups on the outer surface; these modified nanoparticles were named Si-MPS. A polymer shell was grown onto Si-MPS by free radical polymerization of MOI. In a typical preparation, 0.1 g of Si-MPS were dispersed in 4 mL of THF and then AIBN (4 wt% with respect to the monomer) was added as initiator. After 2.5 h of mixing at room temperature to promote AIBN adsorption onto Si-MPS, the suspension was centrifuged and the residual reintroduced in THF solution containing MOI at different concentration, namely 0.85, 2.10, 2.70 or 3.35 M. The polymerization was carried out under N_2 atmosphere at 60 °C for 24 h. After polymerization, the silica nanoparticles modified by the polymer shell deriving from MOI polymerization were centrifuged and washed three times with fresh THF in order to eliminate any possible trace of residual unreacted monomer.

Samples were coded following the MOI concentration used for their preparation:

SiO_2@0.85MOI, SiO_2@2.10MOI, SiO_2@2.70MOI and SiO_2@3.35MOI.

2.3. Synthesis of $SiO_2@Y_2O_3$:Eu^{3+} photoluminescent particles

Stoichiometric amounts of Y_2O_3 and Eu_2O_3 were, respectively, dissolved in nitric acid to form $Y(NO_3)_3$ and $Eu(NO_3)_3$ solution. The doping concentration of Eu^{3+} was fixed at 4 mol% in all samples. Silica particles encapsulated in the MOI polymer shell (0.1 g) were dispersed in 20 mL aqueous solution containing yttrium nitrate (16.6×10^{-2} mol/L) and europium nitrate (6.64×10^{-3} mol/L) in order to promote the sequestering of the lanthanide ions by the polymer shell. Vigorous mechanical stirring was applied at a constant temperature of 50 °C for different time up to 100 h. After mixing, the solution was centrifuged and the powder was dried under vacuum. Then the powder was calcined at 750 °C for 2 h in air atmosphere to obtain a complete elimination of the sacrificial polymer shell and to get $SiO_2@Y_2O_3$:Eu^{3+} photoluminescent nanoparticles. The same procedure was applied to bare silica for the preparation of comparison samples.

2.4. Characterization

Identification and analysis of the polymer shell grown onto the silica particles was done by transmission electron microscopy (TEM) using a JEM 2010 instrument (JEOL Oxford Instruments, UK). The samples were prepared by dipping 150-mesh carbon coated copper grids into dispersion solution of the particles in EtOH. The crystal structure of samples was studied by means of X-rays diffraction (XRD, D500 instrument, Siemens, DE) using CuK_α radiation working with 30 kV accelerating voltage, 25 mA current and 2° 2θ/min. Thermogravimetric analyses (TGA) were carried out using a TA TGA 7 instrument under oxygen streaming atmosphere at a heating rate of 20 °C min^{-1} between room temperature and 700 °C. Photoluminescence was studied through the emission and excitation spectra of $SiO_2@Y_2O_3$:Eu^{3+} photoluminescent particles recorded by a Perkin Elmer LS 50 spectrofluorimeter. The amount of lanthanide ions present at the surface of the photoluminescent particles was quantified by X-rays photoemission spectroscopy (XPS). The experiments were carried out in ultra-high-vacuum at a base pressure of 10^{-9} mbar. XPS data were recorded with a double pass Perkin Elmer PHI 15–255 G cylindrical-mirror electron analyzer (CMA) operated at constant pass energy. The axis of the CMA was set to 15° from the sample normal. X-ray photoemission was carried out with non-monochromatic AlK_α photons ($h\nu = 1486.6$ eV) from a Vacuum Generators XR3 dual anode source operated at 15 kV, 18 mA.

Carbon 1s (C_{1s}), oxygen 1s (O_{1s}), silicon 2p (Si_{2p}), yttrium 3d (Y_{3d}), europium 3d (Eu_{3d}) core level scans were recorded with a resolution of 1 eV, using a pass energy of 50 eV. Quantitative analysis of surface composition was made through the evaluation of the photoemission peak areas, I, of C_{1s}, O_{1s}, Si_{2p}, Y_{3d} and Eu_{3d} and using appropriate empirical atomic sensitivity factors (ASF). The relative atomic concentration of i element (C_i) can be obtained through the relation reported in Eq. (1):

$$C_i = \frac{I_i/ASF_i}{\sum_j (I_j/ASF_j)} \quad (1)$$

The values of ASF depend on the kind of the analyzer and therefore are characteristic for each instrument. A list of ASF to be used for the double-pass cylindrical-mirror

analyzer supplied by Physical Electronics is reported in the Handbook of X-ray Photoelectron Spectroscopy [26]. Inductively coupled plasma mass spectrometry (ICP) was performed using a Liberty 200 instrument (Varian) under standard experimental conditions.

3. Results and discussion

3.1. Silica particles encapsulated in the sacrificial polymer shell

The thermal properties of SiO_2@MOI core shell nanoparticles obtained with different concentrations of MOI (namely 0.85 and 3.35 M) were evaluated by TGA and DSC measurements. The curves of the relative decomposition processes and enthalpic variations are, respectively, reported in Fig. 1((a) and (b)). As expected, a correlation between the weight loss and thickness of the polymer shell was found; the weight loss for bare silica (10 wt%) was increased up to approximately 60 wt% for SiO_2@3.35MOI sample.

The TGA of SiO_2@MOI samples presents different peaks: the weight reduction between room temperature and 200 °C can be attributed to the elimination of residual solvents, water and ethanol formed by condensation reaction of a fraction of silanol groups and ethoxy groups. The weight decrease between 250 and 400 °C is attributed to methacrylate decomposition [27]. The peak at 400 °C is probably due to the overlapping of the contributions from methacrylate to further reaction of the residual silanol groups. The peak at 539 °C can be attributed to a small fraction of residual highly crosslinked polymer formed by the reaction of amine and isocyanate with MPS on silica surface.

This observation also confirms that the amount of polymer grafted onto MPS-modified silica is fairly high. It is very positive for its task of entangling the highest possible amount of lanthanides ions which are precursors of the photoluminescent Y_2O_3:Eu^{3+} shell to be created on the silica cores.

Table 1 shows the correlation between concentration of MOI and average thickness of the obtained polymer shell on silica core. As the monomer concentration during the polymerization was increased from 0.85 to 3.35 M, the thickness of polymer shell also increased linearly from ~23 to ~55 nm, respectively. This caused that the average thickness of yttria shell increased from ~12 to ~22 nm ,respectively, (compare pictures (c) of Figs. 4–7).

Table 1
Correlation between concentration of MOI and average thickness of the obtained polymer shell on silica core.

Sample	MOI concentration (M)	sacrificial polymer shell thickness (nm)	yttria shell thickness after calcination (nm)
SiO_2@0.85MOI	0.85	23	7
SiO_2@2.10MOI	2.10	38	12
SiO_2@2.70MOI	2.70	45	18
SiO_2@3.35MOI	3.35	55	22

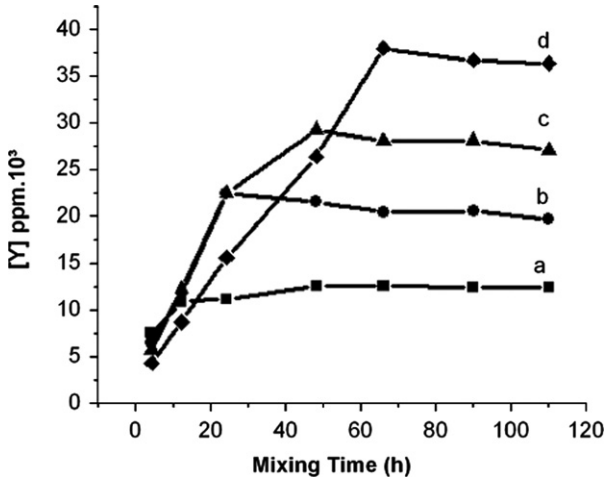

Fig. 2. Amounts of Y^{3+} ions adsorbed by (a) bare silica and core shell samples with (b) 0.85 M MOI, (c) 2.7 M MOI and (d) 3.35 M MOI at different mixing times.

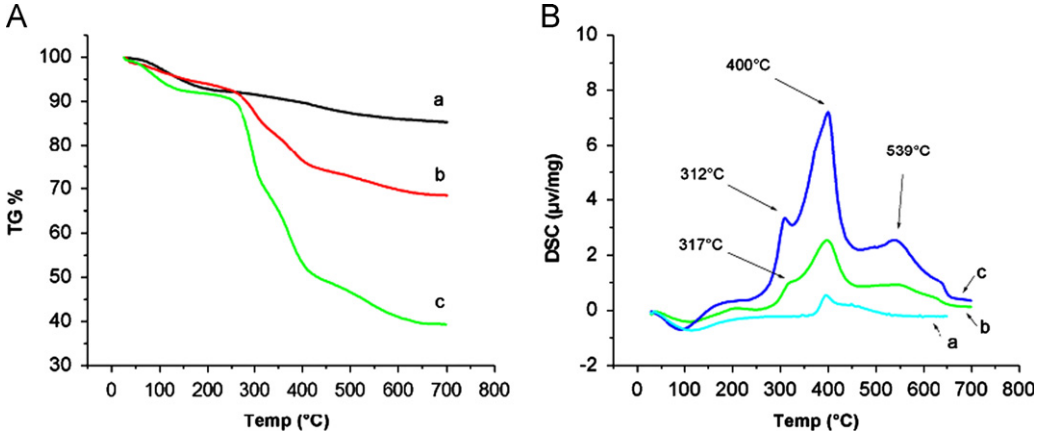

Fig. 1. TGA (A) and DSC (B) curves of bare silica (a), core shell samples with 0.85 MMOI (b) and 3.35 MMOI (c).

3.2. Sequestering of lanthanide ions and formation of the luminescent shell onto silica cores

In order to evaluate the capability of the polymer shell to capture Y^{3+} (Eu^{3+}) ions, the $SiO_2@Y_2O_3:Eu^{3+}$ core–shell particles were mixed in HNO_3 solution for 24 h. In this situation, Y_2O_3 dissolves and turns to yttrium nitrate, while silica remains unchanged. The ICP test was done on the extracting solutions, in order to evaluate the amount of Y^{3+} ions released by the shell layers. Results reported in Fig. 2 show that the amount of Y^{3+} ions released by the $Y_2O_3:Eu^{3+}$ shell increases by increasing the time of mixing in yttrium nitrite solution, and with increasing thickness of the sacrificial polymer shell used to prepare the $SiO_2@Y_2O_3:Eu^{3+}$ hybrid particles, which in turn is related to the increasing concentration of MOI. This represents a proof of the fundamental role played by the sacrificial polymer shell for capturing the highest possible amount of Y^{3+} ions responsible for a highly homogeneous and bright photoluminescent shell.

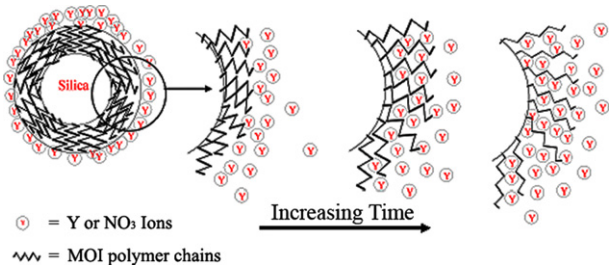

Fig. 3. Schematic representation of the role played by the polymer shell in adsorption of Y^{3+} and Eu^{3+} ions.

As schematically represented in Fig. 3, the polymer shell reaches higher degrees of swelling by increasing the time of mixing in yttrium nitrate, thus allowing a higher diffusion of Y^{3+} and Eu^{3+} ions towards the silica cores; these ions will be also stabilized by the polymer chains [25] and this will positively affect the homogeneity, thickness and adhesion of the lanthanide shell. As attended, thicker polymer shells deriving from higher concentrations of MOI need longer time to swell.

By TEM micrographs reported in Figs. 4–7, the role played by the thickness of the sacrificial polymer shell on the final lanthanide layer can be directly observed.

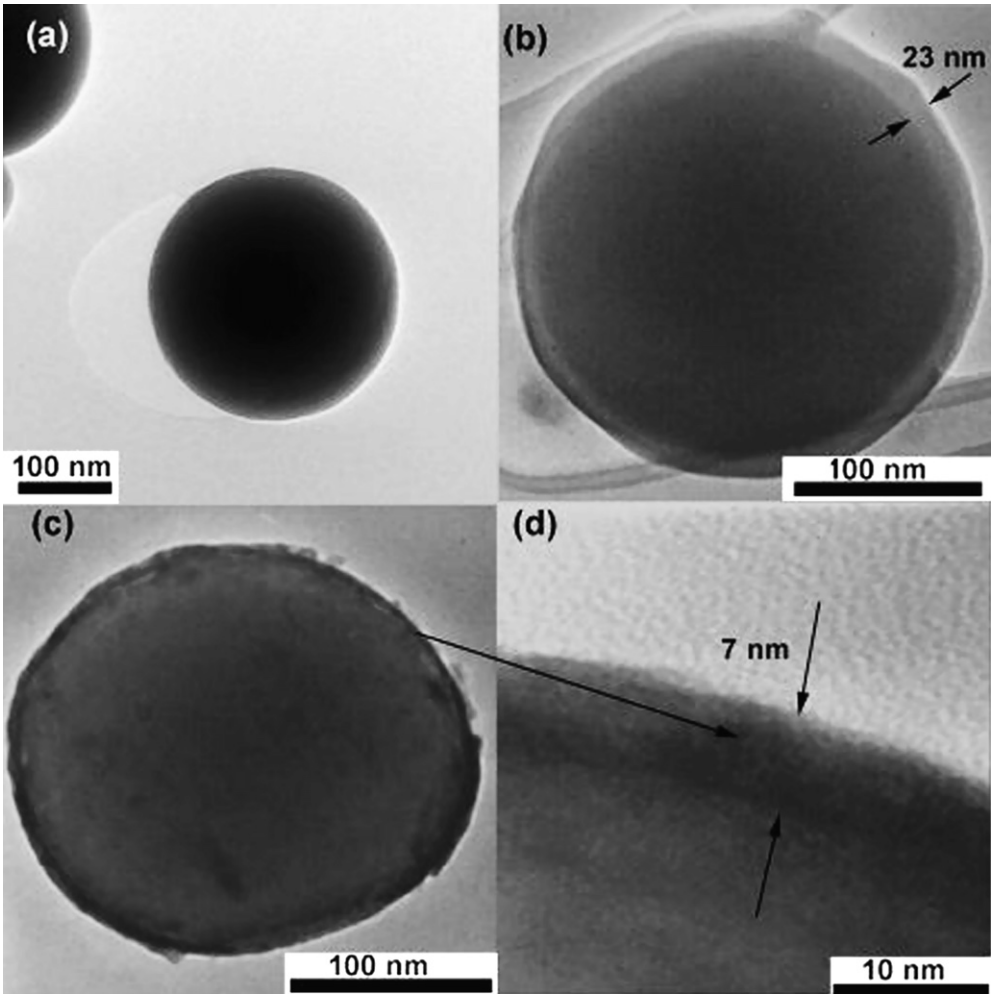

Fig. 4. TEM micrographs of (a) bare silica, (b) silica grafted with 0.85 M MOI and ((c) and (d)) silica@$Y_2O_3:Eu^{3+}$ obtained from silica grafted with 0.85 M MOI after calcination for polymer removal.

The pristine bare silica nanoparticle is shown in Fig. 4(a) and (b) shows the particles modified by surface-initiated polymerization of MOI for the creation of a sacrificial polymer shell (SiO_2@0.85MOI). The latest allowed to obtaining homogeneous photoluminescent Y_2O_3:Eu^{3+} layers on the silica cores (Fig. 4(c)), approximately 7 nm thick (Fig. 4(d)).

Analogous images are reported in Fig. 5((a)–(d)) for SiO_2@Y_2O_3:Eu^{3+} hybrid particles were deriving from SiO_2@2.10MOI, in Fig. 6((a)–(d)) for hybrid particles were deriving from SiO_2@2.70MOI and finally in Fig. 7((a)–(d)) for hybrid particles were deriving from SiO_2@3.35MOI.

The HRTEM micrographs (Fig. 5(d) and Fig. 6(d)) clearly indicate the lattice fringes of the crystalline phase of Y_2O_3 located on the shell of silica cores. Also, the electron diffraction patterns of SiO_2@Y_2O_3:Eu^{3+} derived from SiO_2@3.35MOI shown in Fig. 7(d) demonstrate that the shell contains nanocrystalline domains.

Therefore, the sacrificial polymer shell method allows the formation of a more homogeneous and thicker layer of photoluminescent oxide onto the silica cores, confirming that the polymer act as adsorbent medium due to its amine, amide and urea groups which during the mixing with yttrium nitrate solution attract and stabilize Y^{3+} ions [25]. Furthermore, the thermal removal of the sacrificial polymer shell does not affect the adhesion of the luminescent shell to the silica core.

The XRD patterns of SiO_2@Y_2O_3:Eu^{3+} photoluminescent particles prepared with and without the sacrificial polymer shell are reported in Fig. 8. All samples were calcinated at 750 °C. As it can be noticed, the position of all the main characteristic peaks (at 2θ values of 29.160, 48.541 and 57.9) in the samples matches to those of the reference pattern (JCPDS reference No. 83-927). However there are differences in the intensity of peaks, which increases by increasing the thickness of the polymer shell on silica particles.

3.3. Photoluminescence

Finally, in order to find a correlation between the optical properties (intensity of photoluminescence) of the prepared core–shell particles, and their structural features, a quantitative evaluation of the amount of yttrium atoms at the surface of the particles has been done by XPS analysis.

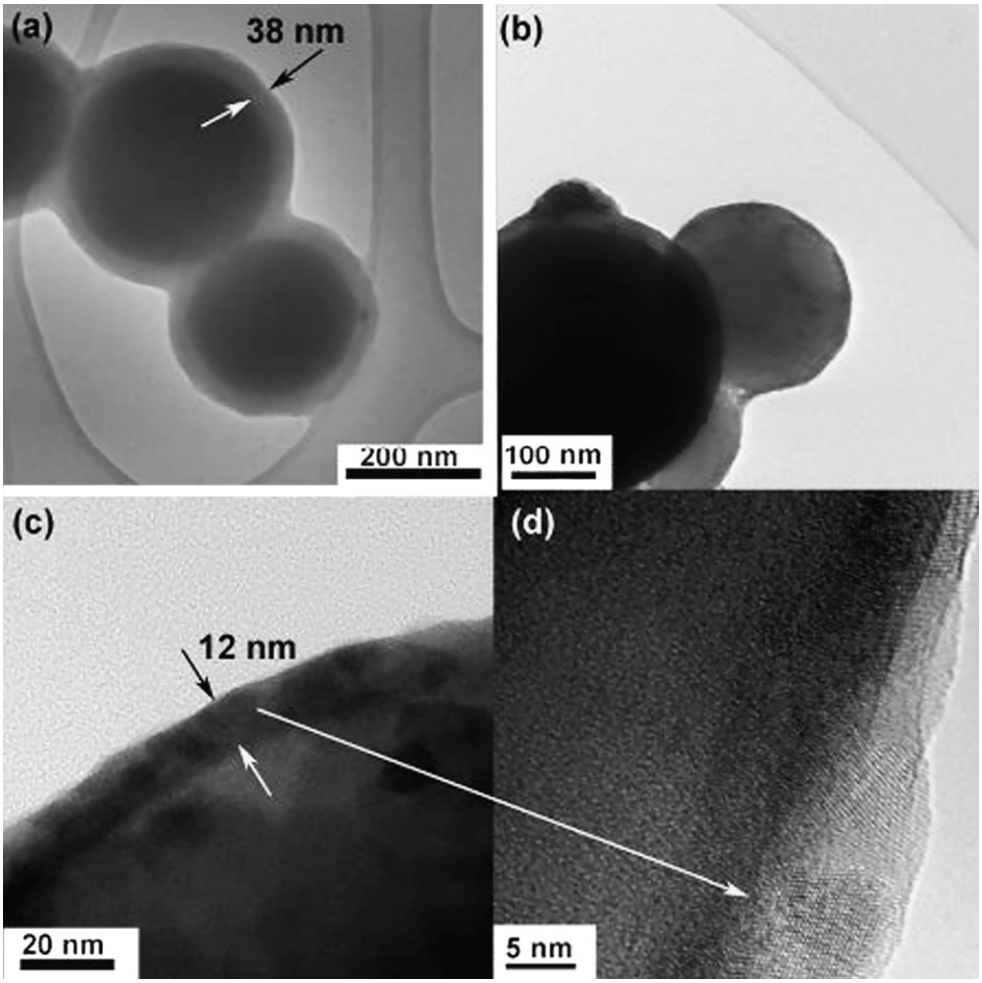

Fig. 5. TEM micrographs of silica grafted with 2.1 M MOI (a), SiO_2@Y_2O_3:Eu^{3+} obtained by silica grafted with 2.1 M MOI ((b) and (c)) after calcination for polymer removal and HRTEM from the yttria shell (d).

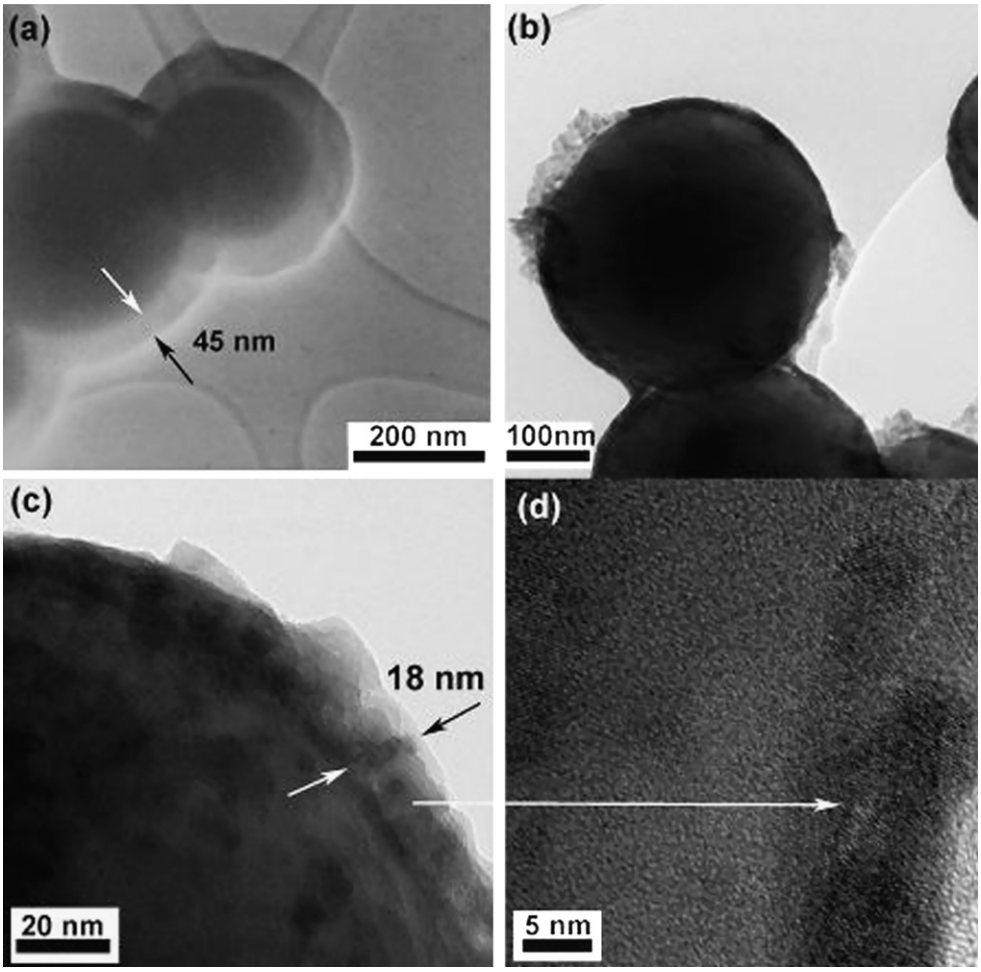

Fig. 6. TEM micrographs of silica grafted with 2.7 M MOI (a), $SiO_2@Y_2O_3:Eu^{3+}$ obtained by silica grafted with 2.7 M MOI ((b) and (c)) after calcination for polymer removal and HRTEM from the yttria shell (d).

Results are reported in Table 2 for bare silica (a), $SiO_2@Y_2O_3:Eu^{3+}$ prepared without polymer shell (b), and with a sacrificial polymer shell having different thickness, namely 23 nm (SiO_2@0.85MOI (c)) and 55 nm (SiO_2@3.35MOI (d)).

These results reveal that the sacrificial polymer shell method (samples (c) and (d)), allows the stabilization of higher amounts of yttrium atoms in the shell around silica cores; the polymer shell thickness plays an important role, higher concentration reflecting in higher amounts of Y ions present at the surface.

Fig. 9(a)–(c) shows, respectively, the XPS spectra of Y_{3d}, Si_{2p} and O_{1s} of bare silica cores and silica@$Y_2O_3:Eu^{3+}$ samples. In particular, in Fig. 9(a), the Y_{3d} spectra are shown for samples (b)–(d) of Table 2. The spectra present two structures, which can be associated to the Y_{3d} peak at 158.7 eV and to the Si_{2s} emission at 153.5 eV from the silica cores. The energy resolution does not allow to disentangle the 5/2–3/2 spin orbit splitting of the Y peak. Its energy position is compatible with oxidized Y [28]. It is noteworthy that the Si_{2s} emission does not disappear even at the high shell thickness of sample (d), which could indicate some incomplete or inhomogeneous coverage. This is consistent with Fig. 9(b), in which the evolution of the Si_{2p} peak is shown. The Si levels are initially at about 102.9 eV for both bare silica (a) and silica@$Y_2O_3:Eu^{3+}$ prepared without polymer shell samples (b). A binding energy shift of 0.7 eV towards lower binding energy is observed for samples (c) and (d). This can be related to a reaction between Si and yttria in the form of Si–O–Y chemical bonds [29]. Concerning O_{1s} emission (Fig. 9(c)) bare silica cores present a prominent structure at 533 eV, which is consistent with literature [28,30]. A minor lower binding energy structure could be related to some traces of hydrocarbon contamination. As long as the core particles are covered with yttria, a low binding energy component at about 530 eV increases, which can be associated to Y–O bonding in the oxide [28,30]. The main component at 532.5 eV can be assigned to Si–O–Y bond formation on the silica surface [28,30] with contribution from the Si–O bonding of the silica cores, which cannot be separated at the used energy resolution.

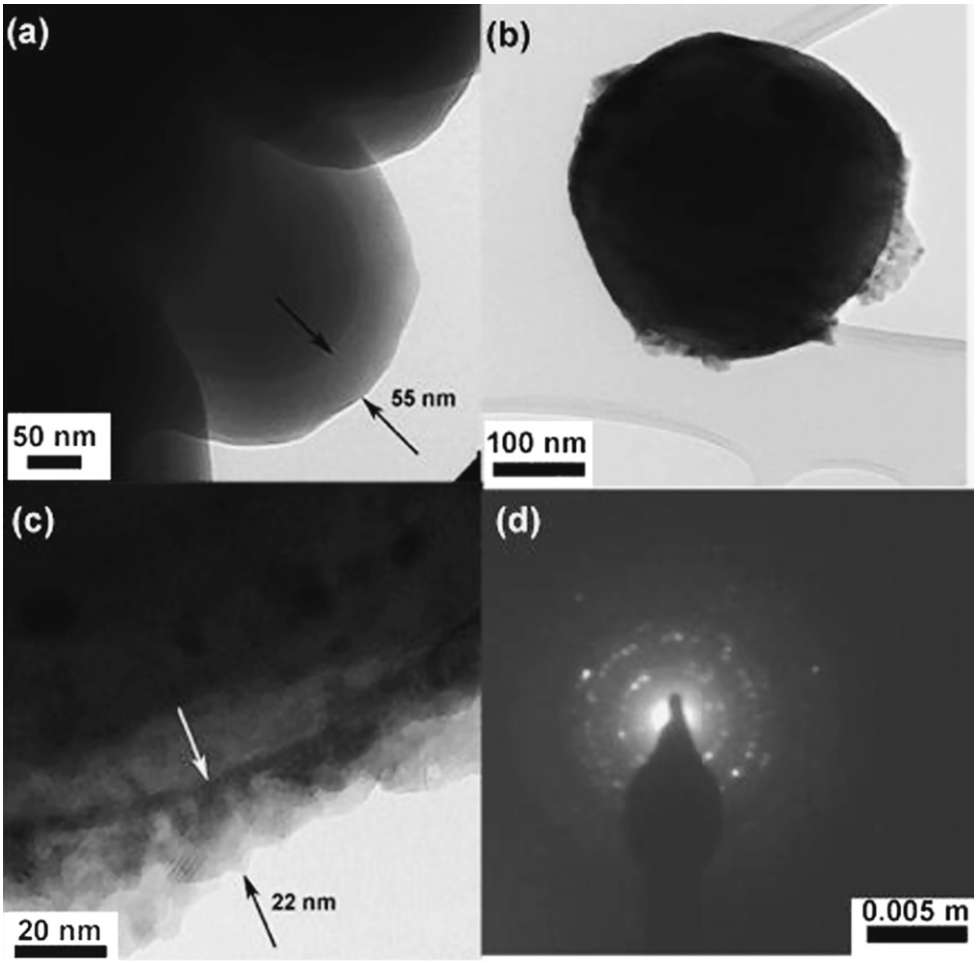

Fig. 7. TEM micrographs of silica grafted with 3.35 M MOI (a), $SiO_2@Y_2O_3:Eu^{3+}$ obtained by silica grafted with 3.35 M MOI ((b) and (c)) after calcination for polymer removal and diffraction pattern from the shell (d).

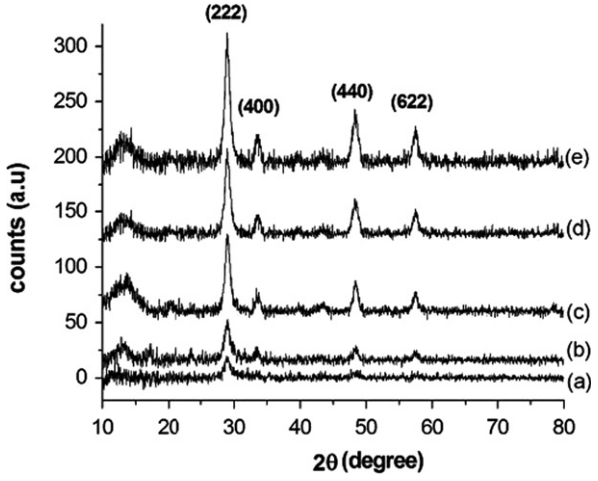

Fig. 8. XRD patterns of $SiO_2@Y_2O_3:Eu^{3+}$ photoluminescent particles prepared with or without the sacrificial polymer shell, at different MOI concentration. (a): Without sacrificial polymer shell, (b): silica@ Yttria:Eu^{3+},0.85 M MOI, c: silica@ Yttria:Eu^{3+},2.1 M MOI, d: silica@ Yttria:Eu^{3+},2.7 M MOI, (e): silica@ Yttria:Eu^{3+},3.35 M MOI.

Table 2
XPS quantitative evaluation of Y atoms at the surface of core–shell particles.

sample	% Si	%Y	%Eu
a	28	0	0
b	28	6	traces < 1%
c	14	12	traces < 1%
d	12	17	traces < 1%

Fig. 10 shows the excitation (a) and emission (b) spectra of $SiO_2@Y_2O_3:Eu^{3+}$ core–shell particles synthesized by the sacrificial polymer shell method, compared to analogous particles prepared without polymer intermediate.

The intensity of photoluminescence results is impressively higher for core–shell particles prepared through the sacrificial polymer shell method and it increases by increasing the polymer shell thickness.

It is clear that just the characteristic emission line ($^5D_0$-$^7F_2$) is present in the $SiO_2@Y_2O_3:Eu^{3+}$ (0% MOI)

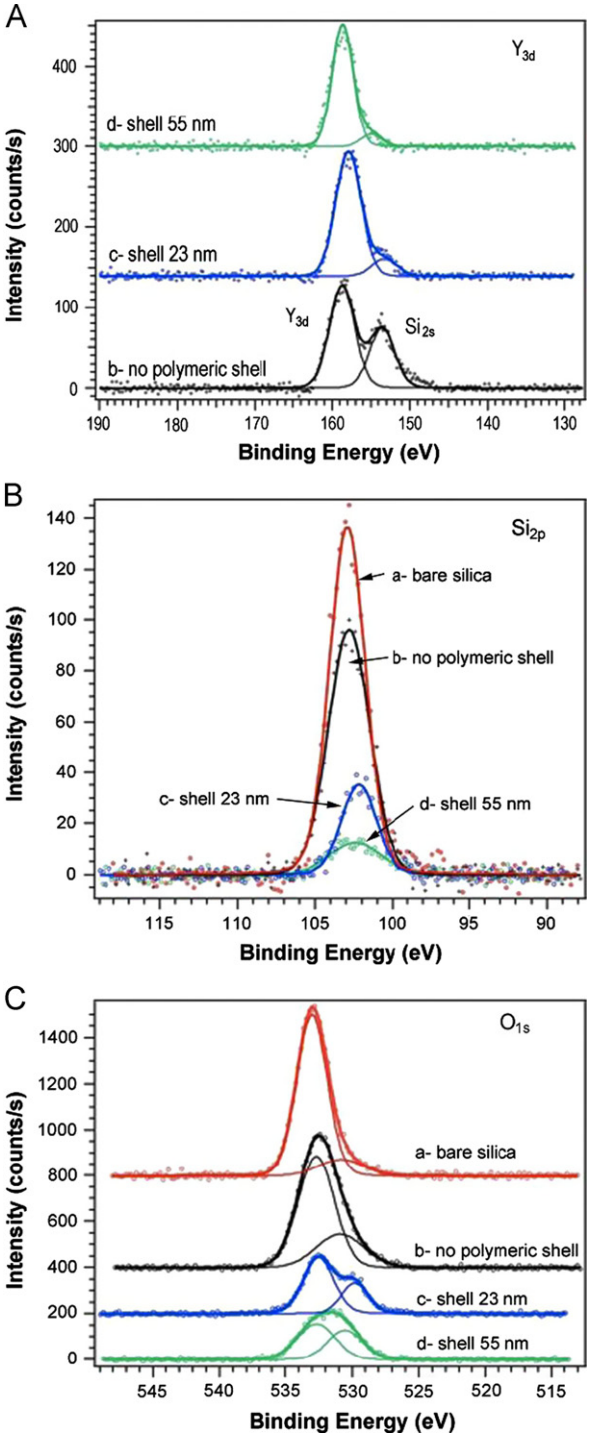

Fig. 9. Y_{3d} (A), Si_{2p} (B) and O_{1s} (C) XPS spectra of bare silica (a), $SiO_2@Y_2O_3:Eu^{3+}$ prepared without polymer shell (b), and with a sacrificial polymer shell method that monomer concentration was 0.85 (c) and 3.35 M (d). The spectra were decomposed in single voigt components, according to a least square fitting, after a Shirley background subtraction.

spectrum, while the most characteristic emission lines ($^5D_0$-^7F_j, $J=1$, 2, 3) are present in the spectra obtained for particles prepared with the polymer shell [31,32]. Furthermore, there are no intense excitation peaks for particles prepared without the polymer shell due to low

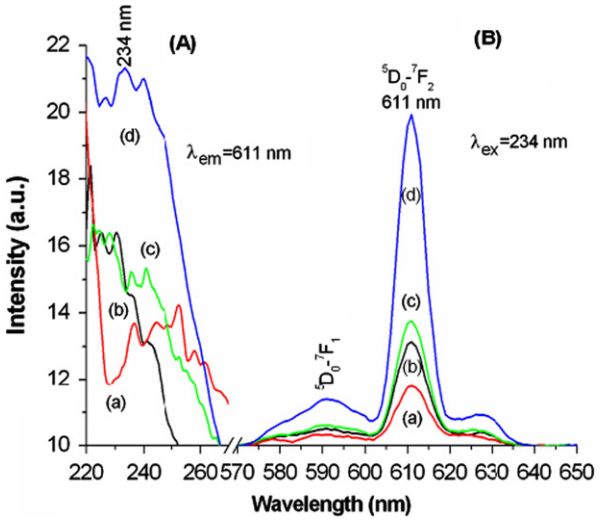

Fig. 10. Excitation (A) and emission (B) spectra of $SiO_2@Y_2O_3:Eu^{3+}$ samples, (a): silica@ Yttria:Eu^{3+}, 0% MOI, (b): silica@ Yttria:Eu^{3+},0.85 M MOI, (c): silica@ Yttria:Eu^{3+},2.1 M MOI, (d): silica@ Yttria:Eu^{3+}, 3.35 M MOI.

amount of yttria on silica particles. But, the maximum excitation level belongs to $SiO_2@Y_2O_3:Eu^{3+}$(3.35 M MOI) sample. The intensity of maximum peak is located at 234 nm. This peak is assigned to the charged-transfer band of Eu^{3+} which corresponds to the electronic transition from the 2p orbital of O^{2-} to the 4f orbital of Eu^{3+} [33]. $Y_2O_3:Eu^{3+}$ shell is responsible for luminescent intensity. In other hand, the XRD and TEM results revealed that crystallinity and amount of yttria on silica core are higher for sample prepared by polymer shell method than normal one. Therefore, the luminescent intensity of $SiO_2@Y_2O_3:Eu^{3+}$ from $SiO_2@3.35MOI$ is the highest because of the highest thickness of lanthanide shell [34].

4. Conclusions

Silica particles with poly (methacryl oxyethyl isocyanate) chains grafted on vinyl groups introduced on silica by chemical modification with 3-(trimethoxysilyl) propyl methacrylate, have been successfully prepared by direct free radical polymerization. These silica particles having a highly homogeneous polymer shell of different thickness have been mixed for different times with THF solutions of lanthanide ions (Y^{3+}, Eu^{3+}) in order to promote their sequestering. Calcination at 750 °C induced the complete thermal degradation of the sacrificial polymer shell, and the achievement of a highly homogeneous $Y_2O_3:Eu^{3+}$ shell (thickness up to 22 nm) deposited onto the silica cores. XPS measurements demonstrated that the surface composition of the lanthanide shell is richer in yttrium atoms when core–shell particles are prepared through a sacrificial polymer shell. The presence of higher amount of lanthanides, along with the increased thickness and homogeneity of the shell, reflects in much brighter photoluminescence.

Acknowledgements

Dr. Mauro Zapparoli (CIGS, University of Modena and Reggio Emilia, Italy) is gratefully acknowledged for the TEM images.

References

[1] V.A. Bolchouchine, E.T. Goldburt, B.N. Levonovitch, V.N. Litchmanova, N.P. Sochtine, Designed, highly-efficient FED phosphors and screens, Journal of Luminescence 87–89 (2000) 1277–1279.

[2] H. Wang, C.K. Lin, X.M. Liu, J. Lin, M. Yu, Monodisperse spherical core–shell-structured phosphors obtained by functionalization of silica spheres with Y_2O_3:Eu^{3+} layers for field emission displays, Applied Physics Letters 87 (2005) 181907–181910.

[3] T. Ye, Z. Guiwen, Z. Weiping, X. Shangda, Combustion synthesis and photoluminescence of nanocrystalline Y_2O_3:Eu phosphors, Materials Research Bulletin 32 (1997) 501–506.

[4] N. Vu, T.K. Anh, G.C. Yi, W. Strek, Photoluminescence and cathodoluminescence properties of Y_2O_3:Eu nanophosphors prepared by combustion synthesis, Journal of Luminescence 122–123 (2007) 776–779.

[5] C. Kim, Il-Eok Kwon, C.H. Park, Y.J. Hwang, H.S. Bae, B.Y. Yu, C.H. Pyun, G.Y. Hong, Phosphors for plasma display panels, Journal of Alloys and Compounds 311 (2000) 33–39.

[6] Yanjie Liang, Jun Ouyang, Hongyou Wang, Weili Wang, Pengfei Chui, Kangning Sun, Synthesis and characterization of core–shell structured SiO_2@YVO_4:Yb^{3+},Er^{3+} microspheres, Applied Surface Science 258 (2012) 3689–3694.

[7] G. Li, Z. Wang, Z. Quan, X. Liu, M. Yu, R. Wang, J. Lin, Sol–gel growth of Gd_2MoO_6:Eu^{3+} nanocrystalline layers on SiO_2 spheres (SiO_2@Gd_2MoO_6:Eu^{3+}) and their luminescent properties, Surface Science 600 (2006) 3321–3326.

[8] J. Lin, M. Yu, C. Lin, X. Liu, Multiform oxide optical materials via the versatile pechini-type sol–gel process: synthesis and characteristics, Journal of Physical Chemistry C 111 (2007) 5835–5845.

[9] Jia-Ye Tang, Cheng Zhan, Li-Xun Yang, Lu-Yuan Hao, Xin Xu, Agathopoulos Simeon, synthesis of *h*-BN encapsulated spherical core–shell structured SiO_2@$Sr_2Si_5N_8$:Eu^{2+} red phosphors, Materials Chemistry and Physics 132 (2012) 1089–1094.

[10] W. Stober, A. Fink, E. Bohn, Controlled growth of monodisperse silica spheres in the micron size range, Journal of Colloid and Interface Science 26 (1968) 62–69.

[11] Hye Young Koo, Jang Heui Yi, You Na Ko, Jung Hyun Kim, Yun Chan Kang, Firing characteristics of size-controlled silver–glass composite powders prepared by spray pyrolysis, Powder Technology 198 (2010) 347–353.

[12] Lihua Li, Ruishi Xie, Yongjun Gu, Jinliang Huang, Jianguo Zhu, Preparation and characterization of ZnS:Fe/MX (M=Cd, Zn; X=S, Se) core–shell nanocrystals, Applied Surface Science 258 (2012) 5992–5995.

[13] P.N.R. Kishore, P. Jeevanandam, A novel thermal decomposition approach for the synthesis of silica–iron oxide core–shell nanoparticles, Journal of Alloys and Compounds 522 (2012) 51–62.

[14] Y. Zhang, X.J. Zhang, Q. Tang, D.H. Wu, Z. Zhou, Core–shell VPO_4/C anode materials for Li ion batteries: Computational investigation and sol–gel synthesis, Journal of Alloys and Compounds 522 (2012) 167–171.

[15] F. Zhang, R. Che, X. Li, C. Yao, J. Yang, D. Shen, P. Hu, W. Li, D. Zhao, Direct Imaging the upconversion nanocrystal core/shell structure at the subnanometer level: shell thickness dependence in upconverting optical properties, Nano Letters 12 (2012) 2852–2858.

[16] A.V. Malko, Y. Park, S. Sampat, C. Galland, J. Vela, Y. Chen, J.A. Hollingsworth, V.I. Klimov, H. Htoon, Pump-intensity- and shell-thickness-dependent evolution of photoluminescence blinking in individual core/shell CdSe/CdS nanocrystals, Nano Letters 11 (2011) 5213–5218.

[17] T. Liu, W. Xu, X. Bai, H. Song, Tunable silica shell and its modification on photoluminescent properties of Y_2O_3:Eu^{3+}@SiO_2 nanocomposites, Journal of Applied Physics 111 (2012) 064312.

[18] H. Wang, M. Peng, J. Zheng, P. Li, Encapsulation of silica nanoparticles by redox-initiated graft polymerization from the surface of silica nanoparticles, Journal of Colloid and Interface Science 326 (2008) 151–157.

[19] X. Ding, J. Zhao, Y. Liu, H. Zhang, Z. Wang, Silica nanoparticles encapsulated by polystyrene via surface grafting and in situ emulsion polymerization, Materials Letters 58 (2004) 3126–3130.

[20] Yunxing Li, Zhaoqun Wang, Hao Gu, Gi Xue, A facile strategy for synthesis of multilayer and conductive organo-silica/polystyrene/polyaniline composite particles, Journal of Colloid and Interface Science 355 (2011) 269–273.

[21] Yuvaraj Haldorai, Won Seok Lyoo, Seok Kyun Noh, Jae-Jin Shim, Ionic liquid mediated synthesis of silica/polystyrene core–shell composite nanospheres by radical dispersion polymerization, Reactive and Functional Polymers 70 (2010) 393–399.

[22] S. Smith, P. Shajesh, T.D.R. Nair, K.G.K. Warrier, Synthesis of biocompatible hydrophobic silica–gelatin nano-hybrid by sol–gel process, Colloids and Surfaces B: Biointerfaces 55 (2007) 38–43.

[23] Qi Gan, Xunyu Lu, Yuan Yuan, Jiangchao Qian, Huanjun Zhou, Xun Lu, Jianlin Shi, Changsheng Liu, A magnetic, reversible pH-responsive nanogated ensemble based on Fe_3O_4 nanoparticles-capped mesoporous silica, Biomaterials 32 (2011) 1932–1942.

[24] Paola Fabbri, Mehdi Ghahari, Francesco Pilati, Touradj Ebadzadeh, Roya Aghababazadeh, Ghasem Kavei, Novel approach to the synthesis of core–shell particles by sacrificial polymer shell method, Materials Letters 64 (2010) 2265–2268.

[25] M. Ghahari, P. Fabbri, T. Ebadzadeh, R. Aghababazadeh, F. Pilati, F.A. Hesari, Synthesis of photoluminescent core–shell silica particles by sacrificial polymer shell method, Nano 5 (2010) 221–229.

[26] B. Vincent Crist, Handbook of Monochromatic XPS Spectra, The Elements of Native Oxides, John Wiley & Sons, 2000.

[27] O. Lam, Y. Hervaud, B. Boutevin, Homopolymerization and copolymerization of isocyanatoethyl methacrylate, Journal of Polymer Science Part A: Polymer Chemistry 44 (2006) 4762–4768.

[28] Zeming Xuerui Cheng, Guobin Qi, Hongjun Zhang, Weiping Zhou, Zhang, Min Yin, Growth and characterization of Y_2O_3 thin films, Physica B: Condensed Matter 404 (2009) 146–149.

[29] Guixia Liu, Guangyan Hong, Synthesis of SiO_2/Y_2O_3:Eu core–shell materials and hollow spheres, Journal of Solid State Chemistry 178 (2005) 1647–1651.

[30] Guixia Liu, Guangyan Hong, Xiangting Dong, Jinxian Wang, Synthesis of Y_2O_3: Eu^{3+} hollow spheres using silica as templates, Journal of Rare Earths 25 (2007) 407–411.

[31] H.S. Yoo, H.S. Jang, W.B. Im, J.H. Kang, D.Y. Jeon, Particle size control of a monodisperse spherical Y_2O_3:Eu^{3+} phosphor and its photoluminescence properties, Journal of Materials Research 22 (2007) 2017–2024.

[32] L. Wang, Y. Pan, Y. Ding, W. Yang, W.L. Mao, S.V. Sinogeikin, Y. Meng, G. Shen, H. k. Mao, High-pressure induced phase transitions of Y_2O_3 and Y_2O_3:Eu^{3+}, Applied Physics Letters 94 (2009) 061921.

[33] L. Tong, D. Liu, L. Shi, X. Yang, H. Yang, Magnetic and luminescent properties of Fe_3O_4@Y_2O_3:Eu^{3+} nanocomposites, Journal of Materials Science 47 (2012) 132–137.

[34] X. Ying, G. Zhi-yong, W. Da-peng, J. Yi, L. Ning, J. Kai, Synthesis and photoluminescence properties of uniform Y2O3:Eu3+ hollow spheres with tunable shell thickness, Chemical Research in Chinese Universities 27 (2011) 919–923.